# Use of static and dynamic $^{18}$F-FDopa PET parameters for detecting patients with glioma recurrence or progression

**Timothée Zaragori**
Université de Lorraine
**Merwan Ginet**
Université de Lorraine, CHRU-Nancy
**Pierre-Yves Marie**
Université de Lorraine, CHRU-Nancy
**Veronique Roch**
Université de Lorraine CHRU-Nancy
**Rachel Grignon**
Université de Lorraine CHRU Nancy
**Guillaume Gauchotte**
Université de Lorraine CHRU Nancy
**Fabien Rech**
Université de Lorraine CHRU Nancy
**Marie Blonski**
Université de Lorraine CHRU Nancy
**Zohra Lamiral**
Université de Lorraine CHRU Nancy
**Luc Taillandier**
Université de Lorraine CHRU Nancy
**Laetitia Imbert**
Université de Lorraine CHRU Nancy
**Antoine Verger** ( a.verger@chru-nancy.fr )
CHRU Nancy https://orcid.org/0000-0003-2194-0328

**Original research**

**Keywords:** 18 F-FDopa, glioma, recurrence, dynamic analysis, amino-acid PET

**Posted Date:** May 19th, 2020

**DOI:** https://doi.org/10.21203/rs.3.rs-17078/v2

**Version of Record:** A version of this preprint was published at EJNMMI Research on May 29th, 2020. See the published version at https://doi.org/10.1186/s13550-020-00645-x.

# Abstract

Background: Static 18 F-FDopa PET images are currently used for identifying patients with glioma recurrence/progression after treatment, although the additional diagnostic value of dynamic parameters remains unknown in this setting. The aim of this study was to evaluate the performances of static and dynamic 18 F-FDopa PET parameters for detecting patients with glioma recurrence/progression as well as assess further relationships with patient outcome.

Methods: Fifty-one consecutive patients who underwent an 18 F-FDopa PET for a suspected glioma recurrence/progression at post-resection MRI, were retrospectively included. Static parameters, including mean and maximum tumor-to-normal-brain (TBR) ratios, tumor-to-striatum (TSR) ratios and metabolic tumor volume (MTV), as well as dynamic parameters with time-to-peak (TTP) values and curve slope, were tested for predicting: 1) glioma recurrence/progression at 6-months after the PET exam and 2) survival on longer follow-up.

Results: All static parameters were significant predictors of glioma recurrence/progression (accuracy≥94%) with all parameters also associated with mean progression-free survival (PFS) in the overall population (all $p<0.001$, 29.7 vs. 0.4 months for TBR max , TSR max and MTV). The curve slope was the sole dynamic PET predictor of glioma recurrence/progression (accuracy=76.5%) and was also associated with mean PFS ($p<0.001$, 18.0 vs. 0.4 months). However, no additional information was provided relative to static parameters in multivariate analysis.

Conclusion: Although patients with glioma recurrence/progression can be detected by both static and dynamic 18 F-FDopa PET parameters, most of this diagnostic information can be achieved by conventional static parameters. Further studies are warranted to investigate the relevance of such 18 F-FDopa kinetics in populations involving only high-grade gliomas.


# Background

Gliomas represent approximately 80% of malignant tumors of the central nervous system (CNS) [1]. These tumors have a poor prognosis with a median overall survival of 15 months for glioblastomas, the most common of glioma entities. This particular poor prognosis partly results from a high risk of recurrence/progression with a median progression free survival (PFS) of only 8 to 11 weeks for high-grade gliomas [2]. Even though magnetic resonance imaging (MRI) remains the gold standard for imaging these tumors, MRI is nonetheless dependent on the disruption of the blood–brain barrier and may hence be limited with regard to the differential diagnosis between residual tumors and post-therapeutic changes in tumors with suspected recurrence [3].

Amino-acid PET has been proposed as a criterion for detecting glioma recurrence by the Response Assessment in Neuro-Oncology (RANO) group [3] and has become a current indication for differentiating glioma recurrence from treatment-induced changes, as stated in the recent joint European Association of

Nuclear Medicine (EANM)/European Association of Neuro-Oncology (EANO)/RANO practice guidelines [4].

$^{18}$F-FDopa PET is an amino acid PET tracer for which the ability to diagnose glioma recurrence has been previously established [5–7]. In particular, $^{18}$F-FDopa PET was found to detect glioma recurrence with an accuracy as high as 82% in a retrospective study of 110 patients, in which the lesion-to-normal-tissue ratio was additionally predictive of PFS [8]. More recently, in a study in which glioma recurrence was proven histologically, $^{18}$F-FDopa PET accuracy was reported to reach 84%, using maximum $^{18}$F-FDopa uptake as diagnostic parameter [9]. This accuracy for detecting glioma recurrence was even higher, reaching 96%, in a prospective, albeit smaller study of 28 patients [10].

However, all of the aforementioned $^{18}$F-FDopa PET studies [5–10] were conducted while solely taking into account static $^{18}$F-FDopa PET parameters whereas information provided by dynamic parameters was not considered. It should be noted that such dynamic parameter-derived information has previously been studied in the assessment of glioma recurrence/progression with another widely used amino-acid radiotracer, O-(2-[$^{18}$F]fluoroethyl)-L-tyrosine ($^{18}$F-FET) [11–14], whereas $^{18}$F-FET and $^{18}$F-DOPA are known to present relatively equal performances [15]. Dynamic $^{18}$F-FDopa parameters have also been used to distinguish high-grade from low grade recurrent gliomas with regard to the World Health Organization (WHO) 2007 classification [16]. Moreover, such parameters were recently found to allow characterizing the molecular features of gliomas according to the WHO 2016 classification [17]. However, it remains unknown whether dynamic parameters may also enhance the diagnostic accuracy of $^{18}$F-FDopa PET prescribed for detecting glioma recurrence/progression.

The aim of the present study was thus to assess the performances of $^{18}$F-Dopa PET with both static and dynamic parameters in detecting patients with progressive or recurrent glioma and for assessing further relationships with patient outcome.

# Materials And Methods

### Patients

From October 2012 to October 2017, 245 patients referred to the Department of Nuclear Medicine at the CHRU Nancy for brain tumor assessment were investigated by $^{18}$F-FDopa PET. Fifty-one of these patients were retrospectively selected on the basis that they had an initial history of surgically-resected glioma and that the considered $^{18}$F-FDopa PET had been prescribed for differentiating recurrence/tumor progression from post-therapeutic effects after a non-contributive MRI. As usual in our department, a minimum delay of 2 months is always respected between the surgery or end of radiotherapy and the performing of $^{18}$F-FDopa PET in order to reduce the risk of $^{18}$F-FDopa PET false positives [18].

In such patients, a clinical follow-up and MRI are systematically performed at least every 3 months or at shorter intervals as clinically indicated after surgery [8]. For the present study, the final diagnosis of

glioma recurrence/progression at 6 months or for further assessment of survival was blinded from the $^{18}$F-FDopa PET results and was based on current guidelines for which a recurrence/progression is the result of any new tumor or brain lesion at MRI and/or clear increase in tumor size or in contrast enhancement, and/or significant clinical deterioration, with all of these criteria not being attributable to other non-tumor causes and not due to steroid tapering [19–21]. Patients with lesions which were classified as therapy-related changes due to the course of the disease did not receive any additional therapy beyond the standard therapy due to suspected recurrence. For 4 patients having undergone stereotactic biopsy or open resection, the diagnosis of recurrence/prognosis was assessed neuropathologically.

The assessment of $^{18}$F-FDopa PET parameters for differentiating recurrence/progression from post-therapeutic effects was based on the evaluation of the previous criteria during a 6-month follow-up period. However, PFS and overall survival (OS) were calculated from the date of the PET exam to the date of definite diagnosis of progression and of death, respectively, with a minimum delay of 19 months of observation. The final date for reporting any event for PFS or OS was June 1$^{st}$, 2019.

The local ethics committee (Comité d'Ethique du CHRU de Nancy) approved the retrospective data evaluation on June 7, 2018, and authorization from the CNIL (National Commission on Information Technology and Civil Liberties) was delivered on June 25, 2018 (authorization n° R2018-11). This study complied with the principles of the Declaration of Helsinki. Informed consent was obtained from all individuals included in the study.

## Initial pathological grading of the gliomas

All cases were reviewed and classified according to the WHO 2016 classification from tumor samples provided by surgery or stereotactic biopsy [22]. IDH mutation status was assessed by immunohistochemistry with IDH1 R132H protein expression (Dianova, clone H09), or by Sanger sequencing in case of ATRX immunohistochemical loss without IDH1 R132H staining [23]. Tumors presenting oligodendroglial morphology or showing IDH mutation without ATRX loss were additionally tested for 1p/19qco-deletion using multiplex PCR fragment analysis (loss of heterozygosity), or comparative genomic hybridization [24].

## PET recordings and image reconstruction

$^{18}$F-FDopa PET-computed tomography (CT) scans were obtained on a Biograph hybrid system involving a six-detector CT for attenuation correction (Biograph 6 True Point, SIEMENS, Erlangen, Germany). Patients were instructed to fast for at least 4 hours with some patients also receiving Carbidopa administration one hour prior to their exam (n = 17). The CT scan was recorded first and immediately followed by a 30-

min 3D list-mode PET recording initiated during the bolus injection of 3 MBq of $^{18}$F-FDopa per kilogram of body weight. The static PET images were reconstructed from the list mode data ranging from 10 to 30 min post-injection [4,7] while the PET images reconstructed for dynamic parameters encompassed 6 consecutive frames of 20 sec each followed by 28 frames of 1 min each. The choice of this acquisition time frame was based on previous studies performed with $^{18}$F-FET PET (from 0 to 40 minutes post-injection with a reconstructed 20- to 40-min static image [25]) and on the maximum observed uptake of $^{18}$F-FDOPA in a PET study involving high-grade and low-grade gliomas (respectively 8 and 10 minutes post-injection) [26].

All static and dynamic images were reconstructed with an OSEM 2D algorithm (2 iterations, 21 subsets, 4-mm Gaussian post-reconstruction filter), corrected for attenuation, scatter and radioactive decay, and displayed in a 256x256 matrix with 2.7x2.7x3.0 mm$^3$ voxels.

## Analyses of PET images

Regions of interest (ROIs) were placed on the static PET images using a dedicated software (DOSIsoft, Cachan, France). A spherical ROI of 2 cm diameter, centered on the maximum lesion uptake, was used for determining maximum and mean Standardized Uptake Values ($SUV_{max}$ and $SUV_{mean}$, respectively). Tumor-to-striatum (TSR) and tumor-to-normal-brain (TBR) ratios were computed as $SUV_{mean}$ or $SUV_{max}$ of the lesion uptake divided by the $SUV_{mean}$ of the striatum ($TSR_{mean}$ and $TSR_{max}$) or of normal brain ($TBR_{mean}$ and $TBR_{max}$). The $SUV_{mean}$ from the striatum was obtained from the contralateral basal ganglia, which was segmented using a threshold of 65% of maximal uptake, while the normal reference brain $SUV_{mean}$ was obtained with a crescent shape ROI (2x8 cm) positioned on the semi oval center of the unaffected contralateral hemisphere, including white and grey matter [4].

When no abnormal $^{18}$F-FDopa uptake was detected, the ROIs of the potential residual tumor were placed at the site of maximal MRI abnormalities with a fused display of PET and Fluid Attenuation Inversion Recovery (FLAIR) MRI images [7].

As previously described [27], the metabolic tumor volume (MTV) was obtained through a 3D auto-contouring process with a threshold corresponding to the $SUV_{mean}$ of the contralateral striatum.

In addition, time-activity curves, representing the evolution of the $TBR_{mean}$ as a function of time ($TAC_{ratio}$), were extracted with the PLANET® Dose software (DOSIsoft, Cachan, France) and with the ROIs previously placed on static images (see above). Each dynamic frame was previously registered on the CT images, in order to take into account potential patient movements during acquisitions [28]. Two dynamic parameters were determined from fitted curves to overcome noise effects, using a method already validated for $^{18}$F-FET in the same setting [29], namely: i) Time-To-Peak (TTP), corresponding to the delay

between the onset of the dynamic acquisition (time of tracer injection) and the time-point of the maximal $TBR_{mean}$ value, and ii) slope, calculated with a linear regression applied from the $10^{th}$ to $30^{th}$ minute.

### Statistical analysis

Categorical variables are expressed as percentages and continuous variables as median and interquartile range due to the non-normality of variable distributions.

*Recurrence/progression at 6 months follow-up*

Univariate analysis was performed using Mann-Whitney tests applied between patients with glioma recurrence/progression and the remaining patients. In order to calculate diagnostic performances, the optimal threshold for each static and dynamic PET parameter was determined from ROC curves using the maximal value of the product of sensitivity and specificity. Thereafter, a multivariable logistic regression model with forward selection was performed for predicting patients with glioma recurrence/progression.

*Progression-free survival (PFS) and Overall survival (OS)*

The dichotomized parameters, which were determined according to previously mentioned optimal thresholds, were used in survival analyses. For this purpose, univariate survival probabilities according to the Kaplan-Meier method with the log-rank test used and the hazard ratio interval of each parameter with its 95% confidence interval were calculated to compare survival curves.

P-values obtained in univariate analysis as well as in survival analysis were adjusted using Benjamini-Hochberg correction in order to reduce the risk of false discovery [30]. P-values lower than 0.05 were considered as significant.

Analyses were performed with SPSS (SPSS Statistics for Windows, Version 20.0. Armonk, NY: IBM Corp) and R (R Foundation for Statistical Computing, Vienna, Austria).

## Results

### Patient characteristics and follow-up data

The study population included 51 patients with a median age of 50.8 [44.4-59.0] years, 23 of whom were women. According to the 2016 WHO classification for gliomas [22], 8 gliomas (16%) had been initially classified as IDH-mutant astrocytomas (including 2 with anaplastic component), 6 (12%) as IDH-wildtype astrocytomas (including 2 with anaplastic component), 12 (24%) as IDH-mutant and 1p/19q co-deleted oligodendrogliomas (including 4 with anaplastic component), 22 (43%) as IDH-wildtype glioblastomas (GBM) and 3 (6%) as IDH-mutant GBM. Median delay times from the date of surgery to the $^{18}$F-FDopa

PET exam and from the date of the non-contributive MRI to the PET exam were 12.7 [5.9-23.5] months and 16 [7-30] days, respectively.

After the subsequent 6-month follow-up period, 34 patients were ultimately considered as having a recurrent or progressive glioma (3 IDH-mutant astrocytomas, 6 IDH-wildtype astrocytomas, 6 IDH-mutant and 1p/19q co-deleted oligodendrogliomas, 17 IDH-wildtype GBM and 2 IDH-mutant GBM) with 4 cases exhibiting a second recurrence and 2 cases a third recurrence. The remaining 17 patients were thus considered to exhibit only treatment-related changes at MRI. Patient characteristics are detailed in Table 1 as well as in the supplemental Table.

With regard to the location of tumor recurrence, 94% (32/34) were observed in the area of the resection cavity whereas the remaining 6% (2/34) were located remotely.

During an observation period of 41 [23-50] months following the PET exam, 22 patients (43%) died and 43 (84%) had evidence of tumor progression. In the overall population, median survival was 24 [14-43] months.

### PET prediction of glioma recurrence/progression

As detailed in Tables 2 and 3, all studied PET parameters, except TTP, were significant univariate predictors of glioma recurrence/progression (all adjusted $p<0.001$), with a global diagnostic accuracy of 96% being reached with $TBR_{max}$, $TSR_{max}$ and MTV. Meanwhile, the curve slope was the sole significant dynamic PET predictor, although its predictive value was somewhat lower than that obtained with the other PET predictors (-i.e. with a lower area under the ROC curve and with a global diagnostic accuracy of only 76.5%, as detailed in Table 3).

On multivariate analysis, $TSR_{max}$ was the only parameter selected by the model to predict glioma recurrence/progression, with no other dynamic or static PET parameter able to provide any significant additional predictive information (Table 4).

When separating the gliomas into two groups according to their respective grade at initial diagnosis [22], all of the static parameters as well as the curve slope were able to discriminate recurrent or progressive gliomas in initially classified high-grade gliomas (n=33, $p \leq 0.001$) whereas the slope parameter was not discriminative in low-grade gliomas (n=18, $p=0.13$) (Figure 1).

### PET parameters for predicting PFS and OS

All PET parameters, except TTP, were also significant predictors of PFS on Kaplan-Meier analyses, although none were predictive of OS (adjusted p-value=1). More precisely, PFS times were much longer in patients with vs. those without a $TBR_{max} \leq 1.61$ (29.7 vs. 0.4 months; log-rank test adjusted $p<0.001$; hazard ratio (HR) = 7.45 [2.39;23.21], $p<0.01$), a $TBR_{mean} \leq 1.3$ (27.8 vs. 0.5 months; log-rank test adjusted $p<0.001$; HR = 5.81 [2.04;16.53], $p<0.01$), a $TSR_{max} \leq 1.0$ (29.7 vs. 0.4 months; log-rank test

adjusted p<0.001; HR = 7.45 [2.39;23.21], p<0.01), a $TSR_{mean} \leq 0.083$ (25.6 vs. 0.0 months; log-rank test adjusted p<0.001; HR = 6.0 [1.83;19.63], p=0.01), a MTV ≤ 0.045 mL (29.7 vs. 0.4 months; log-rank test adjusted p<0.001; HR = 7.45 [2.39;23.21], p<0.01), or a curve slope ≥ -0.26 $h^{-1}$ (18.0 vs. 0.4 months; log-rank test adjusted p<0.001; HR = 2.45 [1.18;5.07], p=0.03).The corresponding survival curves are depicted in Figure 2.

Representative examples of patients with or without glioma recurrence/progression investigated with $^{18}$F-FDopa imaging are provided in Figure 3.

# Discussion

In the present population of patients with suspected glioma recurrence/progression at post-resection MRI, both static and dynamic $^{18}$F-FDopa PET parameters were significant predictors of a glioma recurrence/progression at 6-months, as well as of progression-free survival on the longer term. This diagnostic information was however mostly achieved with conventional static parameters, with limited additional diagnostic information provided by dynamic parameters, contrary to that previously reported in the very different clinical setting of newly-diagnosed gliomas [17].

The diagnostic performances of $^{18}$F-FDopa PET imaging in the present study were very high, in keeping with those reported in a previous study [10], reaching a global accuracy of 96% for predicting patients with glioma recurrence/progression at 6-months after the $^{18}$F-FDopa PET exam. This global accuracy is moreover higher when compared with the 82% level previously reported for the $^{18}$F-FDopa PET detection of glioblastoma recurrence in a population of 110 patients [8].

Of particular note, upon multivariate analysis, none of the dynamic parameters were shown to provide any additional diagnostic information, comparatively to that obtained with static parameters. This statement is particularly explain by the high performance values obtained with the static parameters in this setting of suspicion of glioma recurrence/progression (accuracy ≥ 94%).

These results partially support previous results documented for $^{18}$F-FET and in which the univariate predictive values of the dynamic parameters were consistently lower than that of static parameters [11–14]. In particular, in a large study cohort including 124 patients, dynamic $^{18}$F-FET PET parameters (TTP, curve pattern) were less predictive than static parameters ($TBR_{max}$, $TBR_{mean}$) for glioma recurrence/progression [11].

However, the added-value of dynamic parameters appears to be more pronounced in the context of high-grade gliomas only, as previously shown in a study by Fleischmann et al. whereby dynamic $^{18}$F-FET PET parameters displayed a higher prognostic value in tumor recurrences than static parameters [31]. This latter hypothesis is further underscored in the present study in predicting recurrence/progression with dynamic parameters in the high-grade gliomas and not in the low-grade gliomas. Despite the fact that the number of patients was relatively limited, particularly for low-grade gliomas, this finding further

strengthens the fact that dynamic parameters are ostensibly more relevant in instances of high expected uptake, i.e. in high-grade gliomas [5–7], in which a clear decreasing slope in kinetics is typically reported in these most aggressive glioma entities [16,17]. The washout observed in high-grade gliomas, even if still to be well defined, could be related to microvessel density and LAT1 expression but also to the disruption of the blood brain barrier which likely facilitates the initial tumor uptake of the tracers, as well as their subsequent passive backdiffusion [32]. By contrast, lower-grade gliomas preferentially exhibit consistently increasing curves [17,33,34], which are very similar to the $^{18}$F-FDopa time-activity curves expected in normal brain tissue or reactive tissue changes [5]. Thus, the use of dynamic parameters in this setting of low-grade gliomas could hence be more challenging. Another potential rationale is that a sufficiently high tumor uptake is required for an accurate determination of dynamic parameters, whereas this uptake was too low in the present study in cases of an absence of any glioma recurrence/progression (median $TBR_{mean}$=0.84; see Table 2). In contrast to the previous hypotheses, the potential confounding influence of reactive tissue changes, in line with the inflammatory- and healing-processes induced by surgery and/or radiotherapy and/or chemotherapy [35,36] cannot be used to explain the lower diagnostic performances from dynamic parameters. Both static and dynamic parameters should normally be affected in the same manner by the complex histology of the treated sites, involving varying levels of reactive gliosis, inflammatory cells and radiation-induced changes. Moreover, in our clinical practice, $^{18}$F-FDopa PET for detecting glioma recurrence/progression are performed at least 2 months after the surgery or at the end of radiotherapy, limiting the risk of the aforementioned confounding factors.

$^{18}$F-FDopa PET imaging was also predictive of PFS in the present series of suspected recurrent gliomas, with a lower uptake and an increasing slope being associated with a longer PFS (Figure 1). Several studies have observed similar relationships between static amino-acid PET parameters and PFS in recurrent gliomas [8,37–40]. Irrespectively, the data provided herein by $^{18}$F-FDopa PET imaging was furthermore predictive of patient outcome well beyond the 6-month period, reaching up to 18 and 29 months of mean PFS according to dynamic and static parameters, respectively.

The main limitations inherent to this study are that results were obtained retrospectively in a single center. In addition, our sample size was too limited for providing separate analyses according to the different molecular features of the gliomas involved in the present study, whereas it is possible that $^{18}$F-FDopa uptake may vary according to these features [41–44]. Furthermore, the relative low number of histologically-verified cases should lead to consider with caution the very high accuracy reported in this study. The time activity curves of tumors were expressed through ratios with tracer activity from normal brain, a method successfully tested by our team for the detection of newly-diagnosed gliomas [17], along with the necessity to lower the possible interference of Carbidopa premedication [45]. Lastly, the calculation of the PFS and OS may be questioned given that all included gliomas, mixing several entities and especially low- and high-grade gliomas, may have benefited from different therapeutic strategies. Notwithstanding, all applied treatments were performed in keeping with general standards [20,21].

# Conclusion

In summary, this novel study, assessing the relevance of $^{18}$F-FDopa kinetics in the diagnosis of recurrent gliomas shows that patients with a glioma recurrence/progression, occurring remotely after surgery, may be detected by both static and dynamic $^{18}$F-FDopa PET parameters. However, in this population mixing both low- and high-grade gliomas, much of this diagnostic information is achievable by conventional static parameters, contrary to that previously documented for the $^{18}$F-FDopa PET detection of newly-diagnosed gliomas. Further studies are warranted to investigate the relevance of such $^{18}$F-FDopa kinetics in populations involving only high-grade gliomas.

# Abbreviations

PFS: Progression-Free Survival

RANO: Response Assessment in Neuro-Oncology

EANM: European Association of Nuclear Medicine

EANO: European Association of Neuro-Oncology

WHO: World Health Organization

OS: Overall Survival

CT: Computed Tomography

ROI: Region Of Interest

SUV: Standardized Uptake Values

TBR: Tumor-to-normal-Brain Ratio

TSR: Tumor-to-Striatum Ratio

FLAIR: Fluid Attenuation Inversion Recovery

MTV: Metabolic Tumor Volume

TTP: Time-To-Peak

GBM: Glioblastomas

MET: $^{11}$C-methyl-methionine

# Declarations

**Ethics approval and consent to participate:** All procedures performed in studies involving human participants were in accordance with the ethical standards of the institutional and/or national research committee and with the 1964 Helsinki declaration and its later amendments or comparable ethical standards. Written informed consent was obtained from all individual participants included in the study. The local ethics committee (Comité d'Ethique du CHRU de Nancy) approved the retrospective data evaluation on June 7, 2018, and authorization from the CNIL (National Commission on Information Technology and Civil Liberties) was delivered on June 25, 2018 (authorization n° R2018-11).

**Consent for publication:** Not applicable

**Availability of data and materials:** All data generated or analyzed during this study are included in this published article and its supplementary information files.

**Competing interests:** All authors declare that they have no competing interests.

**Funding:** None

**Authors' contributions:** All authors participated either to: 1) study conception and design or analysis and interpretation of the data, or both (TZ, MG, VR, ZL, AV); 2) the drafting of the manuscript or its critical revision for important intellectual content (TZ, MG, FR, MB, GG, PYM, LI, AV) or 3) final approval of the submitted manuscript (FR, MB, GG, LT, LI, AV).

**Acknowledgements:** Not applicable

# References

1. Ostrom QT, Gittleman H, Fulop J, Liu M, Blanda R, Kromer C, et al. CBTRUS Statistical Report: Primary Brain and Central Nervous System Tumors Diagnosed in the United States in 2008-2012. Neuro-Oncol. 2015;17 Suppl 4:iv1–62.
2. Lamborn KR, Yung WKA, Chang SM, Wen PY, Cloughesy TF, DeAngelis LM, et al. Progression-free survival: An important end point in evaluating therapy for recurrent high-grade gliomas. Neuro-Oncol. 2008;10:162–70.
3. Albert NL, Weller M, Suchorska B, Galldiks N, Soffietti R, Kim MM, et al. Response Assessment in Neuro-Oncology working group and European Association for Neuro-Oncology recommendations for the clinical use of PET imaging in gliomas. Neuro-Oncol. 2016;18:1199–208.
4. Law I, Albert NL, Arbizu J, Boellaard R, Drzezga A, Galldiks N, et al. Joint EANM/EANO/RANO practice guidelines/SNMMI procedure standards for imaging of gliomas using PET with radiolabelled amino acids and [18F]FDG: version 1.0. Eur J Nucl Med Mol Imaging. 2019;46:540–57.
5. Chen W, Silverman DHS, Delaloye S, Czernin J, Kamdar N, Pope W, et al. 18F-FDOPA PET imaging of brain tumors: comparison study with 18F-FDG PET and evaluation of diagnostic accuracy. J Nucl Med. 2006;47:904–11.

6. Fueger BJ, Czernin J, Cloughesy T, Silverman DH, Geist CL, Walter MA, et al. Correlation of 6-18F-Fluoro-L-Dopa PET Uptake with Proliferation and Tumor Grade in Newly Diagnosed and Recurrent Gliomas. J Nucl Med. 2010;51:1532–8.
7. Janvier L, Olivier P, Blonski M, Morel O, Vignaud J-M, Karcher G, et al. Correlation of SUV-Derived Indices With Tumoral Aggressiveness of Gliomas in Static 18F-FDOPA PET: Use in Clinical Practice. Clin Nucl Med. 2015;40:e429–35.
8. Herrmann K, Czernin J, Cloughesy T, Lai A, Pomykala KL, Benz MR, et al. Comparison of visual and semiquantitative analysis of 18F-FDOPA-PET/CT for recurrence detection in glioblastoma patients. Neuro-Oncol. 2014;16:603–9.
9. Youland RS, Pafundi DH, Brinkmann DH, Lowe VJ, Morris JM, Kemp BJ, et al. Prospective trial evaluating the sensitivity and specificity of 3,4-dihydroxy-6-[18F]-fluoro-L-phenylalanine (18F-DOPA) PET and MRI in patients with recurrent gliomas. J Neurooncol. 2018;137:583–91.
10. Karunanithi S, Sharma P, Kumar A, Khangembam BC, Bandopadhyaya GP, Kumar R, et al. 18F-FDOPA PET/CT for detection of recurrence in patients with glioma: prospective comparison with 18F-FDG PET/CT. Eur J Nucl Med Mol Imaging. 2013;40:1025–35.
11. Galldiks N, Stoffels G, Filss C, Rapp M, Blau T, Tscherpel C, et al. The use of dynamic O-(2-18F-fluoroethyl)-l-tyrosine PET in the diagnosis of patients with progressive and recurrent glioma. Neuro-Oncol. 2015;17:1293–300.
12. Verger A, Filss CP, Lohmann P, Stoffels G, Sabel M, Wittsack H-J, et al. Comparison of O-(2-18F-Fluoroethyl)-L-Tyrosine Positron Emission Tomography and Perfusion-Weighted Magnetic Resonance Imaging in the Diagnosis of Patients with Progressive and Recurrent Glioma: A Hybrid Positron Emission Tomography/Magnetic Resonance Study. World Neurosurg. 2018;113:e727–37.
13. Pyka T, Hiob D, Preibisch C, Gempt J, Wiestler B, Schlegel J, et al. Diagnosis of glioma recurrence using multiparametric dynamic 18F-fluoroethyl-tyrosine PET-MRI. Eur J Radiol. 2018;103:32–7.
14. Maurer GD, Brucker DP, Stoffels G, Filipski K, Filss CP, Mottaghy FM, et al. $^{18}$ F-FET PET imaging in differentiating glioma progression from treatment-related changes – a single-center experience. J Nucl Med. 2020;61:505-11.
15. Lapa C, Linsenmann T, Monoranu CM, Samnick S, Buck AK, Bluemel C, et al. Comparison of the amino acid tracers 18F-FET and 18F-DOPA in high-grade glioma patients. J Nucl Med Off Publ Soc Nucl Med. 2014;55:1611–6.
16. Schiepers C, Chen W, Cloughesy T, Dahlbom M, Huang S-C. 18F-FDOPA Kinetics in Brain Tumors. J Nucl Med. 2007;48:1651–61.
17. Ginet M, Zaragori T, Marie P-Y, Roch V, Gauchotte G, Rech F, et al. Integration of dynamic parameters in the analysis of 18F-FDopa PET imaging improves the prediction of molecular features of gliomas. Eur J Nucl Med Mol Imaging. 2019
18. Sala Q, Metellus P, Taieb D, Kaphan E, Figarella-Branger D, Guedj E. 18F-DOPA, a clinically available PET tracer to study brain inflammation? Clin Nucl Med. 2014;39:e283-285.

19. Wen PY, Macdonald DR, Reardon DA, Cloughesy TF, Sorensen AG, Galanis E, et al. Updated response assessment criteria for high-grade gliomas: response assessment in neuro-oncology working group. J Clin Oncol. 2010;28:1963–72.
20. Weller M, van den Bent M, Hopkins K, Tonn JC, Stupp R, Falini A, et al. EANO guideline for the diagnosis and treatment of anaplastic gliomas and glioblastoma. Lancet Oncol. 2014;15:e395-403.
21. Weller M, van den Bent M, Tonn JC, Stupp R, Preusser M, Cohen-Jonathan-Moyal E, et al. European Association for Neuro-Oncology (EANO) guideline on the diagnosis and treatment of adult astrocytic and oligodendroglial gliomas. Lancet Oncol. 2017;18:e315–29.
22. Louis DN, Perry A, Reifenberger G, von Deimling A, Figarella-Branger D, Cavenee WK, et al. The 2016 World Health Organization Classification of Tumors of the Central Nervous System: a summary. Acta Neuropathol (Berl). 2016;131:803–20.
23. Perizzolo M, Winkfein B, Hui S, Krulicki W, Chan JA, Demetrick DJ. IDH Mutation Detection in Formalin-Fixed Paraffin-Embedded Gliomas Using Multiplex PCR and Single-Base Extension: IDH1/2 Mutation Detection by SNaPshot®. Brain Pathol. 2012;22:619–24.
24. Isal S, Gauchotte G, Rech F, Blonski M, Planel S, Chawki MB, et al. A high 18F-FDOPA uptake is associated with a slow growth rate in diffuse Grade II–III gliomas. Br J Radiol. 2018;91:20170803.
25. Verger A, Stoffels G, Bauer EK, Lohmann P, Blau T, Fink GR, et al. Static and dynamic 18F–FET PET for the characterization of gliomas defined by IDH and 1p/19q status. Eur J Nucl Med Mol Imaging. 2018;45:443–51.
26. Kratochwil C, Combs SE, Leotta K, Afshar-Oromieh A, Rieken S, Debus J, et al. Intra-individual comparison of 18F-FET and 18F-DOPA in PET imaging of recurrent brain tumors. Neuro-Oncol. 2014;16:434–40.
27. Schwarzenberg J, Czernin J, Cloughesy TF, Ellingson BM, Pope WB, Grogan T, et al. Treatment Response Evaluation Using 18F-FDOPA PET in Patients with Recurrent Malignant Glioma on Bevacizumab Therapy. Clin Cancer Res. 2014;20:3550–9.
28. Ye H, Wong K-P, Wardak M, Dahlbom M, Kepe V, Barrio JR, et al. Automated Movement Correction for Dynamic PET/CT Images: Evaluation with Phantom and Patient Data. Chen K, editor. PLoS ONE. 2014;9:e103745.
29. Ceccon G, Lohmann P, Stoffels G, Judov N, Filss CP, Rapp M, et al. Dynamic O-(2-18F-fluoroethyl)-L-tyrosine positron emission tomography differentiates brain metastasis recurrence from radiation injury after radiotherapy. Neuro-Oncol. 2017;19:281–8.
30. Benjamini Y, Hochberg Y. Controlling the False Discovery Rate: A Practical and Powerful Approach to Multiple Testing. J R Stat Soc Ser B Methodol. 1995;57:289–300.
31. Fleischmann DF, Unterrainer M, Bartenstein P, Belka C, Albert NL, Niyazi M. 18F-FET PET prior to recurrent high-grade glioma re-irradiation-additional prognostic value of dynamic time-to-peak analysis and early static summation images? J Neurooncol. 2017;132:277–86.
32. Pöpperl G, Kreth FW, Herms J, Koch W, Mehrkens JH, Gildehaus FJ, et al. Analysis of 18F-FET PET for grading of recurrent gliomas: is evaluation of uptake kinetics superior to standard methods? J Nucl

Med. 2006;47:393–403.

33. Pöpperl G, Kreth FW, Mehrkens JH, Herms J, Seelos K, Koch W, et al. FET PET for the evaluation of untreated gliomas: correlation of FET uptake and uptake kinetics with tumour grading. Eur J Nucl Med Mol Imaging. 2007;34:1933–42.
34. Lohmann P, Herzog H, Rota Kops E, Stoffels G, Judov N, Filss C, et al. Dual-time-point O-(2-[18F]fluoroethyl)-L-tyrosine PET for grading of cerebral gliomas. Eur Radiol. 2015;25:3017–24.
35. Carideo L, Minniti G, Mamede M, Scaringi C, Russo I, Scopinaro F, et al. 18F-DOPA uptake parameters in glioma: effects of patients' characteristics and prior treatment history. Br J Radiol. 2018;91:20170847.
36. Stegmayr C, Stoffels G, Kops ER, Lohmann P, Galldiks N, Shah NJ, et al. Influence of Dexamethasone on O-(2-[18F]-Fluoroethyl)-L-Tyrosine Uptake in the Human Brain and Quantification of Tumor Uptake. Mol Imaging Biol. 2019;21:168–74.
37. Beppu T, Terasaki K, Sasaki T, Sato Y, Tomabechi M, Kato K, et al. MRI and 11C-methyl-L-methionine PET Differentiate Bevacizumab True Responders After Initiating Therapy for Recurrent Glioblastoma. Clin Nucl Med. 2016;41:852–7.
38. Beppu T, Sato Y, Sasaki T, Terasaki K, Yamashita F, Sasaki M, et al. Comparisons Between PET With 11C-Methyl-L-Methionine and Arterial Spin Labeling Perfusion Imaging in Recurrent Glioblastomas Treated With Bevacizumab. Clin Nucl Med. 2019;44:186–93.
39. Hutterer M, Nowosielski M, Putzer D, Waitz D, Tinkhauser G, Kostron H, et al. O-(2-18F-fluoroethyl)-L-tyrosine PET predicts failure of antiangiogenic treatment in patients with recurrent high-grade glioma. J Nucl Med. 2011;52:856–64.
40. Galldiks N, Rapp M, Stoffels G, Fink GR, Shah NJ, Coenen HH, et al. Response assessment of bevacizumab in patients with recurrent malignant glioma using [18F]Fluoroethyl-L-tyrosine PET in comparison to MRI. Eur J Nucl Med Mol Imaging. 2013;40:22–33.
41. Verger A, Metellus Ph, Sala Q, Colin C, Bialecki E, Taieb D, et al. IDH mutation is paradoxically associated with higher 18F-FDOPA PET uptake in diffuse grade II and grade III gliomas. Eur J Nucl Med Mol Imaging. 2017;44:1306–11.
42. Cicone F, Carideo L, Scaringi C, Arcella A, Giangaspero F, Scopinaro F, et al. 18F-DOPA uptake does not correlate with IDH mutation status and 1p/19q co-deletion in glioma. Ann Nucl Med. 2019;33:295–302.
43. Zaragori T, Guedj E, Verger A. Is IDH mutation status associated with 18 F-FDopa PET uptake? Ann Nucl Med. 2020;1–2.
44. Cicone F, Carideo L, Scaringi C, Minniti G. Reply to Zaragori et al.: "Is IDH mutation status associated with 18 F-FDopa PET uptake." Ann Nucl Med. 2020;1–2.
45. Hoffman JM, Melega WP, Hawk TC, Grafton SC, Luxen A, Mahoney DK, et al. The effects of carbidopa administration on 6-[18F]fluoro-L-dopa kinetics in positron emission tomography. J Nucl Med. 1992;33:1472–7.

# Tables

**Table 1** Patient characteristics

| n=51 | Value |
|---|---|
| **Age** (years) | |
| Median [Range] | 50.8 [21.2;75.3] |
| **Female gender** *n* (%) | 23 (45) |
| **Primary histopathological type** *n* (%) | |
| IDH-mutant astrocytoma | 8 (16) |
| IDH-wildtype astrocytoma | 6 (12) |
| IDH-mutant and 1p/19q co-deleted oligodendroglioma | 12 (24) |
| IDH-wildtype glioblastoma | 22 (43) |
| IDH-mutant glioblastoma | 3 (6) |
| **Histopathological WHO grade of the primary tumor** *n* (%) | |
| II | 18 (35) |
| III | 8 (16) |
| IV | 25 (49) |
| **Primary treatment** *n* (%) | |
| Surgery | 15 (29) |
| Surgery + radiotherapy | 2 (4) |
| Surgery + chemotherapy | 9 (18) |
| Surgery + radiotherapy + chemotherapy | 25 (49) |

*WHO: World Health Organization*

**Table 2** Median [interquartile range] of PET parameters in the overall population as well as comparatively between the 2 groups of patients with or without glioma recurrence or progression.

| meter | Overall | No Recurrence/progression (n=17) | Recurrence/ progression (n=34) | Adjusted P-value |
|---|---|---|---|---|
| *c* | | | | |
| ıax | 2.22 [1.36;3.12] | 1.26 [1.12;1.37] | 2.71 [2.20;3.69] | <0.001 |
| ıean | 1.57 [1.02;2.13] | 0.84 [0.75;1.04] | 1.95 [1.57;2.70] | <0.001 |
| ıax | 1.31 [0.82;1.90] | 0.77 [0.65;0.82] | 1.64 [1.31;2.28] | <0.001 |
| ıean | 0.92 [0.65;1.43] | 0.51 [0.46;0.65] | 1.19 [0.92;1.69] | <0.001 |
| | 1.49 [0.00;8.22] | 0.00 [0.00;0.00] | 5.35 [1.49;15.75] | <0.001 |
| ***mic*** | | | | |
| | 7.70 [3.35;18.65] | 14.53 [1.55;30.00] | 7.67 [4.13;14.62] | 1 |
| | -0.14 [-0.82;0.13] | 0.07 [-0.07;0.31] | -0.59 [-0.94;-0.08] | <0.001 |

*MTV: metabolic tumor volume; TBR: tumor-to-normal brain ratio; TSR: tumor-to-striatum ratio*

**Table 3** Results provided by ROC curve analyses for the PET identification of patients with glioma recurrence or progression.

| | AUC | CI (95%) AUC | Threshold | Sensitivity | Specificity | Accuracy |
|---|---|---|---|---|---|---|
| **$TBR_{max}$** | 0.969 | (0.923-1.0) | 1.61 | 97.1% | 94.1% | 96.0% |
| **$TBR_{mean}$** | 0.983 | (0.956-1.0) | 1.3 | 94.1% | 94.1% | 94.1% |
| **$TSR_{max}$** | 0.976 | (0.939-1.0) | 1.0 | 97.1% | 94.1% | 96.0% |
| **$TSR_{mean}$** | 0.986 | (0.964-1.0) | 0.83 | 91.2% | 100% | 94.1% |
| **MTV** | 0.978 | (0.939-1.0) | 0.045 mL | 97.1% | 94.1% | 96.0% |
| **Slope** | 0.818 | (0.702-0.935) | -0.26 $h^{-1}$ | 67.6% | 94.1% | 76.5% |

*AUC: area under the curve; CI: confidence interval; MTV: metabolic tumor volume; TBR: tumor-to-normal brain ratio; TSR: tumor-to-striatum ratio*

**Table 4** Results of logistic regression for the prediction of recurrence/progression at 6 months after $^{18}$F-FDopa PET.

| Parameter | Coefficient | p-value |
|---|---|---|
| Intercept | -10.179 | 0.001 * |
| $TBR_{mean}$ | - | 0.244 |
| $TBR_{max}$ | - | 0.605 |
| $TSR_{mean}$ | - | 0.116 |
| $TSR_{max}$ | 10.039 | 0.002 * |
| MTV | - | 0.729 |
| Slope | - | 0.380 |

** indicate parameters ultimately included in the final multivariable model*

*MTV: metabolic tumor volume; TBR: tumor-to-normal brain ratio; TSR: tumor-to-striatum ratio*

# Figures

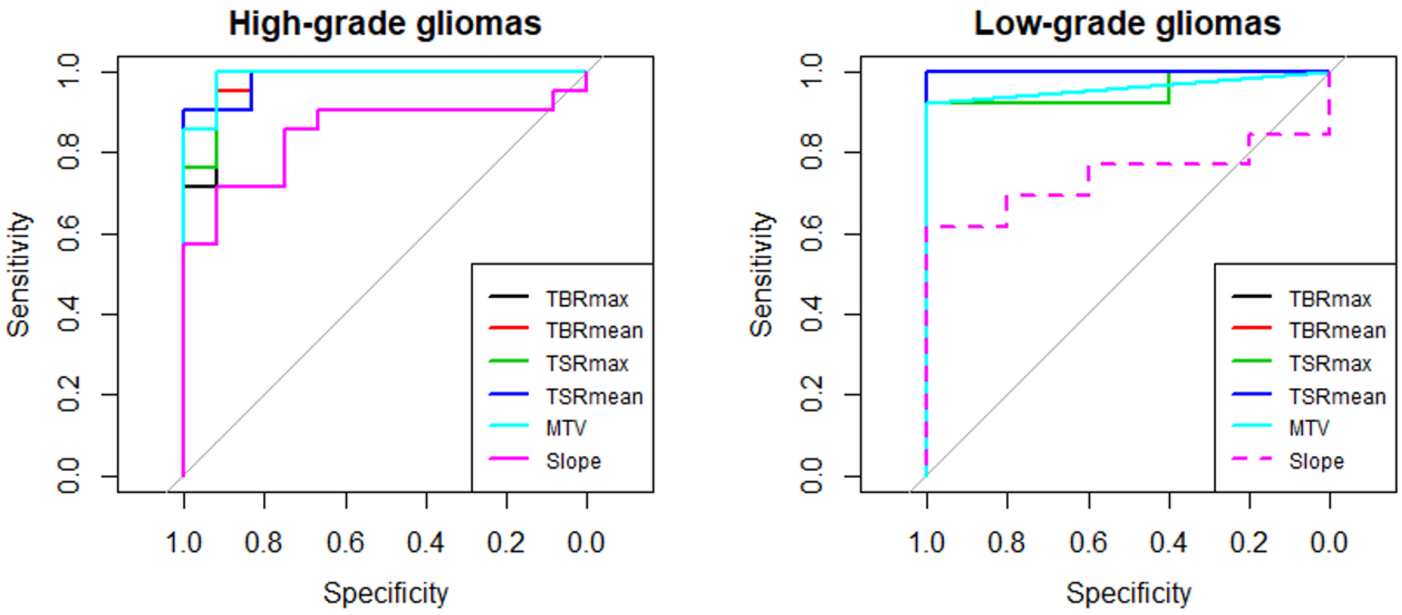


**Figure 1**

Receiver operating characteristic (ROC) curves for TBRmax, TBRmean, TSRmax, TSRmean, MTV and slope parameters for differentiating between recurrent or progressive gliomas and treatment-related changes in high-grade gliomas (n=33, left panel) and in low-grade gliomas (n=18, right panel). Significant ROC curves are represented in solid lines.

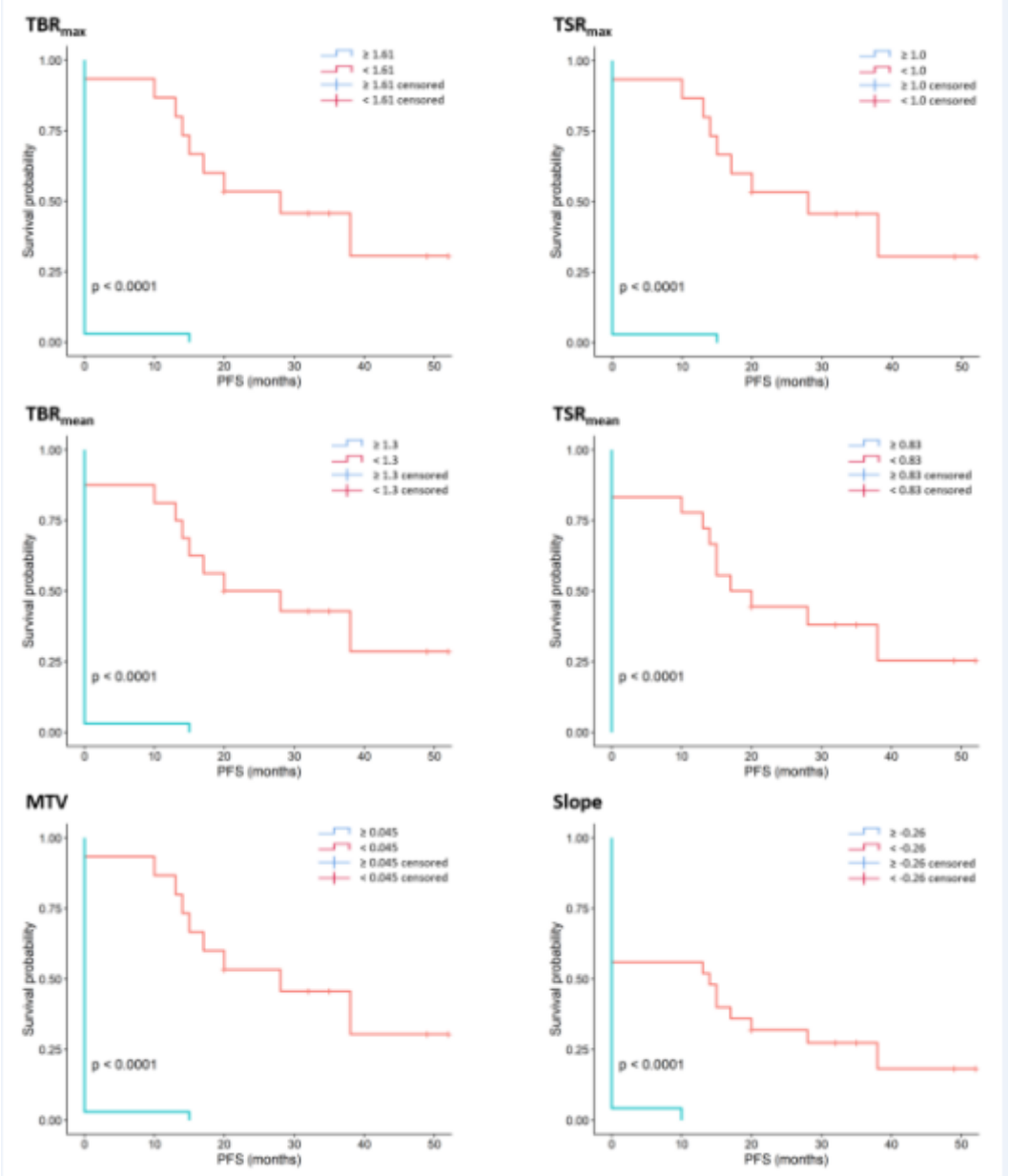


## Figure 2

Kaplan-Meier survival plots for the prediction of progression-free survival using maximal tumor-to-background ratios (upper left panel), mean tumor-to-background ratios (middle left panel), metabolic tumor volume (lower left panel), maximal tumor-to-striatum ratio (upper right panel), mean tumor-to-striatum ratio (middle right panel) and slope (lower right panel) as discriminators. Corresponding log-rank test adjusted p values are <0.0001 for all presented curves.

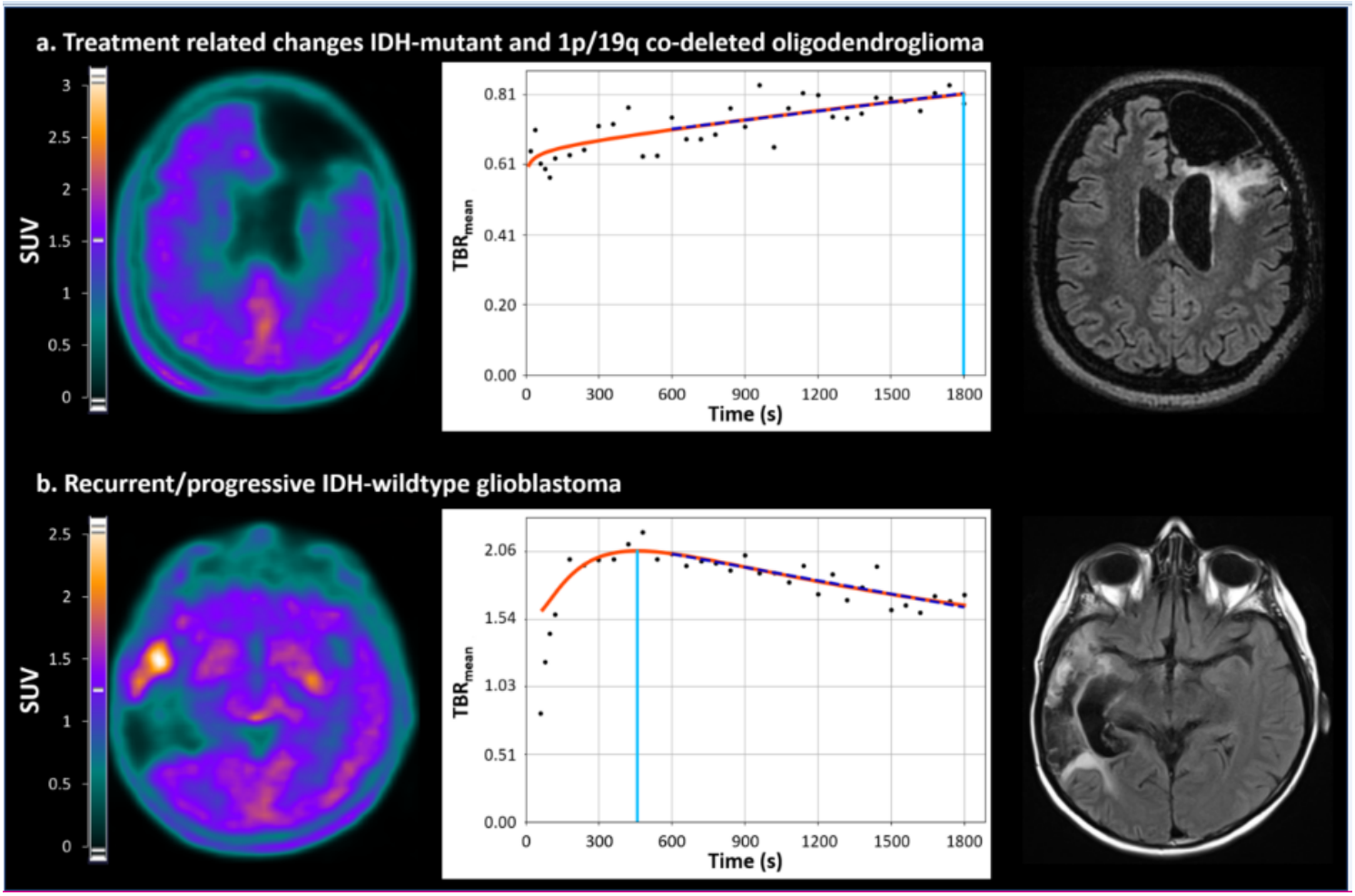


**Figure 3**

Representative examples of patients with or without glioma recurrence/progression investigated with 18F-FDopa imaging, with axial slices of 18F-FDopa PET (left column), dynamic TBRmean curves (middle column) providing the time-to-peak delay-time (light blue dotted line) and the 10-to-30 min slope (dark blue dotted line), along with, for illustrative purposes, the same slice location recorded on a FLAIR MRI sequence (right column). a. 51-year-old woman with no recurrent or progressive glioma (TBRmean=0.8, TBRmax=1.1, TSRmean=0.5, TSRmax=0.7, MTV=0 mL, TTP=30 min and slope=0.31 h-1). b. 46-year-old woman with a progressive IDH-wildtype glioblastoma (TBRmean=1.9, TBRmax=2.5, TSRmean=1.2, TSRmax=1.6, MTV=6.13 mL, TTP=7.6 min and slope=-1.22 h-1).

# Supplementary Files

This is a list of supplementary files associated with this preprint. Click to download.

- SupplementalFigureHD.tiff
- SupplementalFigure.docx
- SupplementalMaterial.xlsx